Arabian Journal of Geosciences (2019) 12: 635
https://doi.org/10.1007/s12517-019-4818-x

ORIGINAL PAPER

Neutron activation and ICP-MS analyses of metals in dust samples—Kingdom of Saudi Arabia: concentrations, pollution, and exposure

Atef El-Taher[1] · Wael M. Badawy[2,3] · B. Alshahrani[4] · Awad A. Ibraheem[1,4]

Received: 9 July 2019 / Accepted: 5 September 2019 / Published online: 16 October 2019
© Saudi Society for Geosciences 2019

Abstract

The present work was conducted to highlight the elemental composition, quantify the extent of pollution, and assess the linked risk due to the exposure to metals in dust samples. The collected samples from Al-Qassim Region were subjected to two complementary analytical techniques: instrumental neutron activation analysis and inductively coupled plasma mass spectrometry. A total of 42 elements were determined, and the concentrations (mg/kg) were compared with the corresponding values from the literature. Considerable concentrations of Br (7.1), Zr (640), Hf (16.5), As (8.9), and Sb (0.7) were observed. Enrichment factor (EF) was calculated to be more than 7 for the same elements, and this a good indicator of a mixed source of pollution with these elements. The integrative pollution index (PI) sorted *Bureydah South* as the strongest contributor of contamination. The exposure assessment showed no hazard risk was observed due to the inhalation of selected elements that distinguished their high toxicity.

Keywords Metals · Dust · NAA · ICP-MS · Pollution · Saudi Arabia

Introduction

The recent study in the Al-Qassim industrial zone showed a marked increase in the overall prevalence rate of non-communicable diseases under the study (cardiovascular diseases, eye and derma problems, respiratory infection, hearing problem, impairment, and diabetes) from 7.1 to 15.7% from the year 2011 to 2015 (Mustafa et al. 2016). Sandstorms increase in April and May due to low pressure in the north of the country. These low pressures or depressions are accompanied with cold fronts that move southeast and cause sandstorms. Dust particles start moving when the horizontal wind speed reaches 20 km per h. In fact, most dust storms start when the speed exceeds 35 km per h. In addition, the ongoing development ignores the local ecosystem.

Crustal aerosol, which is produced from deserts and wadi deposits, plays an important role in the physics and chemistry of the atmosphere. Recently, this key role has been increasingly recognized, and studies of desert aerosol and its atmospheric effects are rapidly increasing. As reported by Rahn et al. (1979), approximately one half of the elements in the atmospheric aerosol occur in near-crustal proportions and are probably soil derived. Deserts are likely to be the main contributors of this crustal dust even to remote temperate and polar regions. Further to that, a large number of elements in the aerosol throughout the troposphere are essentially exclusively controlled by crustal sources. Marine, desert, and anthropogenic aerosols are the main and typical aerosols that exist in Al-Qassim Region, Kingdom of Saudi Arabia. The prevalent of the first two types is attributed to the geographical

Respondible Editor: Domenico M. Doronzo

Electronic supplementary material The online version of this article (https://doi.org/10.1007/s12517-019-4818-x) contains supplementary material, which is available to authorized users.

✉ Atef El-Taher
atef.eltaher@gmail.com

Awad A. Ibraheem
awad_ah_eb@hotmail.com

[1] Department of Physics, Faculty of Science, Al-Azhar University, Assiut Branch, Assiut 71524, Egypt

[2] Department of Radiation Protection & Civil Defense, Nuclear Research Center, Egyptian Atomic Energy Authority (EAEA), Abu Zaabal 13759, Egypt

[3] Frank Laboratory of Neutron Physics, Joint Institute for Nuclear Research, str. Joliot-Curie, 6, Dubna, Moscow Region, Russian Federation 141980

[4] Department of Physics, Faculty of Science, King Khalid University, Abha, Saudi Arabia

location of the country between the Arabian Gulf and large desert areas. Marine aerosols are derived from Arabian Gulf spray, whereas the desert ones are mainly composed of materials such as quartz, calcite, dolomite, feldspars, gypsum, and clay minerals (Ganor et al. 1991; Ganor and Mamane 1982). The anthropogenic aerosols are produced from industrial emissions, power generation, and agriculture. A study of the content of metals in dust and the effect of dust aerosols has attracted the attention of several researchers in the last decades for instance; regionally, a wide-scaled study was conducted, for instance in Kuwait (Al-Awadhi et al. 2014; Al-Dousari 2005, 2009; Al-Dousari et al. 2016, 2017; Al-enezi et al. 2014; Subramaniam et al. 2015), Iraq (Al-Ghadban et al. 2008), and Emirates (Al-Taani et al. 2019; Dan 1990; Ganor 1991; Ganor et al. 1991; Ganor and Mamane 1982; Norouzi et al. 2015; Shaltout et al. 2013). There are many studies regarding dust phenomena globally (Amato et al. 2009; Beavington and Cawse 1979; Blott et al. 2004; Doronzo et al. 2016; Doronzo and Al-Dousari 2019; Khan et al. 1999; Rahn et al. 1979; Rydell and Prospero 1972; Whicker et al. 2006; Zheng et al. 2010).

Therefore, the aim of the present work is the determination of the elemental composition of airborne dust samples and assessment of associated exposure and pollution extent quantification as well. The samples were collected from Al-Qassim Region, Kingdom of Saudi Arabia, and subjected to instrumental neutron activation analysis (INAA) and inductively coupled plasma mass spectrometry (ICP-MS) for analysis. The mentioned analytical techniques are complementary to each other and are distinguished their high accuracy and precision among others.

Materials and methods

Features of the studied area

Al-Qassim Region is one of the thirteen administrative provinces of Saudi Arabia. It is located in the center of Saudi Arabia approximately 400 km northwest of Riyadh. Its area is about 65,000 km^2. Qassim Region has an arid climate, with very hot summer, low rainfall winter, low humidity, and frequent dust storms. A statistical summary of meteorological data for the period of 1985–2010 indicates that the climate in Qassim Region has a mean monthly rainfall of 11.4 mm (Jeddah Regional Centre for Climate 2015). Rain may also occur in the spring, and its rainfall is very rare and normally non-existent. The mean monthly air temperature is 25.1 °C, but winters are much cooler than summer. The mean monthly air temperature is 34 °C and 15 °C, in summer and winter seasons, respectively. During summer, the wind blows dominantly. The average wind speed is 6 kts/month. Dust storms can occur anytime of the year, but they are mostly frequent during March, April, and May and less frequently during the rest of year. Statistical analysis of airborne dust data in Qassim Region shows that blowing dust, dust/sand storm, and haze occur during 34.40%, 6.44%, and 59.15% of the total dusty days, respectively. According to Jeddah Regional Centre for Climate (2015), the blowing dust, dust/sand storms, and rising/suspended dust are continuously present at 29.78% throughout the year in Qassim Region. In addition, statistical analysis shows that the annual average number of dusty days in Qassim Region is 108.7 days (≈ 30% of year).

Sampling and preparation

Fifteen dust samples (total suspended particles) were collected at 1.5 m above ground level from different cities of Al-Qassim Region. The dust samples were collected using dry stainless steel dust fall collectors (squared with the length 1.2 m) modeled on the ASTM standard (A.S.T.M. Standard D-1739-70 1979). The collectors were allocated in some cities in Al-Qassim Region, viz. Shmaceah, Bandareh, Shmaceah East, Bureydah Southeast, Bureydah South, Muleeda South, Muleeda North, Bureydah Center, Bureydah West, Bureydah East, Bureydah North, Bureydah Northeast, Unezah Southeast, Unezah East, and Unezah North as shown in Fig. 1, and the description of the sampling areas is given in Table SM1 (Supplementary material). The samples were collected at the end of the study period (≈ 1 year).

Analytical technique

The prepared samples were analyzed by means of instrumental neutron activation analysis, total digestion ICP, and lithium metaborate/tetraborate fusion ICP. More details on the irradiation and measurement by thermal neutrons at Act Labs in Canada can be found elsewhere by Alharbi and El-Taher (2016) and El-Taher et al. (2003). The analytical parameters of determining packages by INAA and the detection limits are published elsewhere by Hoffman (1992).

For ICP-MS measurement, a 0.25-g sample is digested with four acids beginning with hydrofluoric, followed by a mixture of nitric and perchloric acids, heated using precise programmer–controlled heating in several ramping and holding cycles, which takes the samples to dryness. After dryness is attained, samples were brought back into solution using hydrochloric acid. With this digestion, certain phases may be only partially solubilized. Fused sample is diluted and analyzed by Perkin Elmer Sciex ELAN 6000, 6100, or 9000 ICP/MS. More detail about the treatment of samples for measurement by means of ICP-MS and INAA was published elsewhere (Alharbi and El-Taher 2016; El-Taher and Khater 2016).

Enrichment factor

The abundances of many elements in the atmospheric aerosol are controlled by the crustal aerosol. This can be seen most easily by enrichment factor (EF) analysis, that is, by calculating a normalized enrichment factor of each element in the aerosol relative to the crust. This is usually done for an element by using the following formula (Abrahim and Parker 2008; Badawy et al. 2016, 2017; Lv et al. 2015; Reimann and de Caritat 2005):

$$\mathrm{EF} = (C_x/C_{\mathrm{Sc}})_{\mathrm{aerosol}}/(C_x/C_{\mathrm{Sc}})_{\mathrm{crust}} \quad (1)$$

where $(C_x/C_{\mathrm{Sc}})_{\mathrm{aerosol}}$ is the ratio of the content of the element in the sample and the content of Sc in the sample and $(C_x/C_{\mathrm{Sc}})_{\mathrm{crust}}$ is the ratio of the same reference or background element, which in our case is Sc, in the upper continental crust (UCC) as reported by Rudnick and Gao (2014). Based on the interpretation categories suggested by Ganor et al. (1991), the level of pollution was quantified.

Average single pollution index

In order to estimate the quality of soil and sediments, average single pollution index ($\mathrm{PI}_{\mathrm{avg}}$) was first employed by Qingjie et al. (2008). $\mathrm{PI}_{\mathrm{avg}}$ is defined as

$$\mathrm{PI}_{\mathrm{avg}} = \frac{1}{n}\sum_{i=1}^{n}\mathrm{PI} \quad (2)$$

where n denotes for the number of examined metals and PI is standing for the single pollution index. $\mathrm{PI}_{\mathrm{avg}}$ values higher than unity show a lower soil or sediment quality, which is conditioned by a high contamination level.

Exposure assessment due to dust inhalation

Human exposure pathways of heavy metals to the dust are as follows: (a) direct ingestion of substrate particles (D_{ing}), (b) inhalation of resuspended particles (D_{inh}), and (c) dermal absorption of trace elements to exposed skin (D_{dermal}) or through inhalation of vapors (D_{vapor}) (Zheng et al. 2010). In the present work, a model suggested by US EPA (1996) and Van den Berg (1995) was used to calculate the exposure of adults to the elemental toxicants in dust. The following assumptions and steps underlie the model applied:

a. The chemical risk linked to chemical elements is calculated for some selected elements, viz. Cr, Co, Ni, Cu, Zn, and Pb, because of available inhalation-specific toxicity data (US EPA 1996). The toxicity of Cr is directly dependent on its valence states of Cr(VI) and Cr(III) and the SLF and $R_{\mathrm{f}}D_0$ of Cr(VI) were assumed as for total Cr as stipulated in Table 4 (Kurt-Karakus 2012). As the US EPA has not established an $R_{\mathrm{f}}D_0$ for Pb (US EPA 2010), therefore $R_{\mathrm{f}}D_0$ value used in the calculations in this study was 3.5×10^{-3} mg/kg per day that was calculated from the provisional tolerable weekly Pb intake limit, 25 μg/kg per body weight, recommended by the FAO/WHO for adults (Kurt-Karakus 2012).

b. Chemical daily intake (D_{inh}, mg/kg per day) via inhalation only is considered in the present study and can be given for each element using the following equation (US EPA 1996; Zheng et al. 2010):

$$\mathrm{CDI}_{\mathrm{Inh}} = C_{\mathrm{UCL}}\frac{R_{\mathrm{Inh}} \times F_{\mathrm{exp}} \times T_{\mathrm{exp}}}{\mathrm{PEF} \times A_{\mathrm{BW}} \times T_{\mathrm{avrg}}} \quad (3)$$

The details of the mathematical model, along with the prospective abbreviations and values used in these equations, are specified in Table SM2 (Supplementary material).

C_{UCL} is the exposure, upper confidence limit content in mg kg^{-1}, an estimate of reasonable maximum exposure, and the upper limit at 95% confidence interval of the mean. Since the concentration of most elements in the dust samples has an approximate log-normal distribution, the 95% upper confidence limit (UCL) was calculated using the following equation (US EPA 1996):

$$C_{95\%\mathrm{UCL}} = \exp\left\{\overline{X} + 0.5 \times s^2 + \frac{s \times H}{\sqrt{n-1}}\right\} \quad (4)$$

where $\overline{X}$ is the arithmetic mean of the log-transformed data, s is the standard deviation of the log-transformed data, H is the H statistic, and n is the number of samples (Gilbert 1987).

c. The carcinogenic hazard index (carcinogenic risk (CR)) is a method to estimate the probability of developing cancer in an individual from exposure to trace metals, whereas the non-carcinogenic risk estimates the probability of developing other illnesses. CR is calculated for each metal, using the following equation (Kurt-Karakus 2012; Mohmand et al. 2015; US EPA 2007):

$$\mathrm{CR} = \mathrm{CDI}_{\mathrm{Inh}} \times \mathrm{BAF} \times \mathrm{SLF} \quad (5)$$

The values for the slope factor (SLF), the oral reference dose ($R_{\mathrm{f}}D_0$, mg/kg per day), and the bioaccumulation factor (BAF%) are given in Table 4. The tolerable values for regulatory purposes of the carcinogenic health risk index for different trace metals ranged from 1×10^{-6} to 1×10^{-4} as reported by US EPA (2001).

d. For the studied elements included in the risk analysis, the toxicity reference values considered for the inhalation route are the corresponding oral reference doses ($R_{\mathrm{f}}D_0$, mg/kg per day) and slope factors (SLF). Both are taken

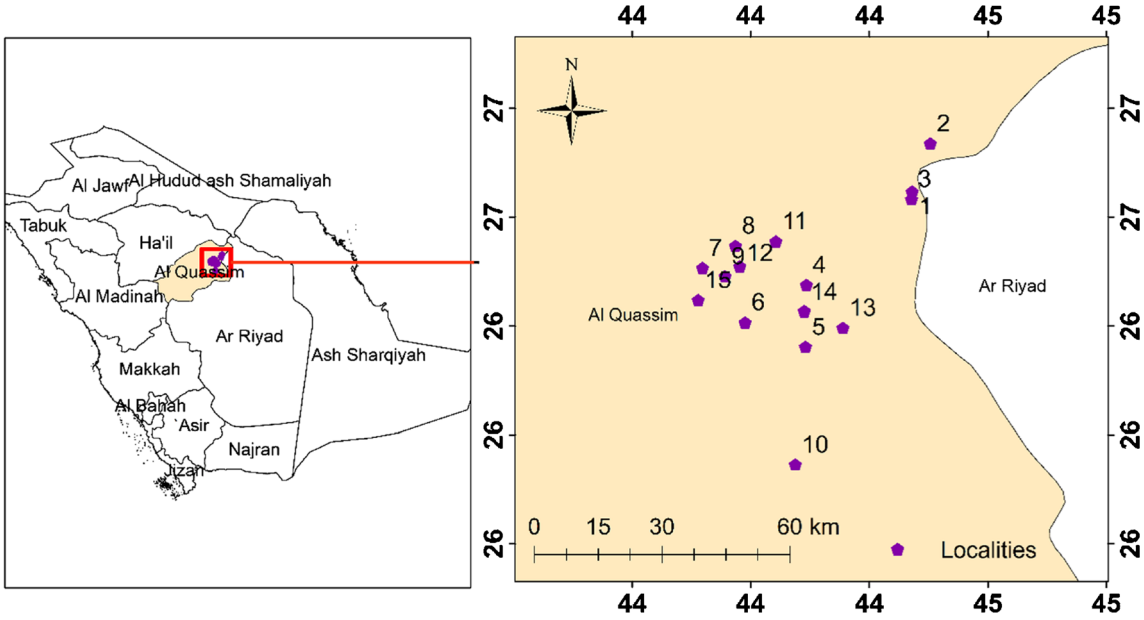

Fig. 1 A map of the studied areas

from Regional Screening Levels tables (US EPA 2017) on the assumption that, after inhalation, the absorption of the particle-bound toxicants will result in similar health effects as if the particles had been ingested. Based on the previous available data and assumptions, the hazard quotient (HQ) was calculated using the following equation:

$$\mathrm{HQ} = (\mathrm{CDI}_{\mathrm{Inh}} \times \mathrm{BAF})/R_{\mathrm{f}}D_0 \quad (6)$$

Finally, the total hazard index is the summation of the hazard quotient.

Statistical analysis

Software packages OriginLab™ Origin 8.5, MS™ Excel, as well as PAST 3.12 (Davis 2002; Hammer et al. 2001) were used for data analysis and graphing. R Programming Environment was used for statistics (R Core Team 2016). Spatial maps were constructed by using ArcGIS.

Results and discussions

Abundance of the elements and inter-correlation

A summary of the descriptive statistics of the obtained concentrations of elements is stipulated in Table 1, as well as the mean, median, standard deviation, minimum, and maximum regarding the distribution of 42 trace elements in dust samples. The results are compared with those published worldwide for the UCC by Rudnick and Gao (2014) and regional published data from dust by Ganor et al. (1991). The Shapiro-Wilk test of normality (Shapiro and Wilk 1965) was calculated where a significance at p value is equal to 0.05. All contents are expressed in mg/kg except S which is given in %. With 95% probability, the normality test show that the total of 42 elements are normally distributed, except that 8 elements are not normally distributed, viz. Be, Cu, Zn, Br, Sn, Sb, Cs, and Pb. All the concentrations of the elements are slightly higher than those averages published worldwide for UCC by Rudnick and Gao (2014) except Be, S, Sc, V, Cr, Co, Ni, Ga, Ge, Sr, Eu, Tl, and Th. For comparison purposes, the results are compared with average published regionally for dust samples by Ganor et al. (1991) and the obtained results are in line as shown in Table 1. The obtained results were normalized and plotted in Fig. 2, relative UCC as reported by Rudnick and Gao (2014). Looking at Fig. 1, considerable concentrations of Br (12.6%) > Zr (7.5%) > Hf (6.9%) > As (5.6%) > Sb (5.5%) are observed and given in descending order.

Based on the normalized concentrations, Fig. 3 is plotted to show three different patterns with respect to regional and worldwide corresponding values. To a great extent, there is a good matching between the obtained results and the corresponding values reported by Ganor et al. (1991) and Hans Wedepohl (1995) and Rudnick and Gao (2003) regionally and worldwide, respectively. Figure 3 can be summarized as follows:

- A group of transition elements includes nine elements such as V, Cr, Co, Ni, Cu, Zn, Y, Hf, and Ta as shown in Fig. 3a. The concentrations (mg/kg) are given for V (85.6 ± 24 with a range of 48–131), Cr (105 ± 25.8 with a range of 57–136), Co (13.2 ± 5.4 with an interval of 5.8–23), Ni

Table 1 Mean, median, standard deviation, minimum, and maximum regarding the distribution of 42 major and trace elements and 11 oxides in airborne dust

Element	Detection limit	Analytical method	Mean	Median	SD	Min	Max	Statistic	*p* value	UCC (Rudnick and Gao 2014)	Dust (Ganor et al. 1991)
Be	1	FUS-ICP	1.53	2.00	0.52	1.00	2.00	0.64	0.000	1.90	1.7
S %	0.001	TD-ICP	0.04	0.03	0.02	0.01	0.08	0.95	0.475	0.04	0.24
Sc	0.01	INAA	10.89	10.30	3.25	5.45	17.40	0.97	0.804	21.90	11
V	5	FUS-ICP	85.60	83.00	24.04	48.00	131.00	0.96	0.762	138.00	97
Cr	0.5	INAA	105.01	113.00	25.78	57.00	136.00	0.91	0.139	135.00	89
Co	0.1	INAA	13.17	11.40	5.41	5.80	23.00	0.93	0.259	26.60	9.5
Ni	1	TD-ICP	52.73	46.00	22.41	26.00	94.00	0.89	0.079	59.00	53.1
Cu	1	TD-ICP	29.80	22.00	18.80	14.00	90.00	0.70	0.000	27.00	42
Zn	1	INAA	72.47	64.00	46.84	33.00	226.00	0.68	0.000	72.00	166
Ga	1	FUS-MS	12.73	12.00	3.59	8.00	19.00	0.91	0.133	16.00	ND
Ge	0.5	FUS-MS	1.18	1.10	0.17	0.80	1.50	0.93	0.313	1.30	ND
As	1	INAA	8.93	9.00	2.69	5.00	15.00	0.94	0.356	2.50	3
Br	0.5	INAA	7.12	3.90	9.75	0.50	38.40	0.68	0.000	0.88	10.2
Rb	1	FUS-MS	60.60	61.00	8.93	44.00	72.00	0.92	0.218	49.00	41
Sr	2	FUS-ICP	251.73	252.00	48.39	182.00	341.00	0.95	0.500	320.00	379
Y	1	FUS-ICP	24.93	25.00	3.45	18.00	31.00	0.98	0.957	19.00	23
Zr	1	FUS-ICP	639.73	694.00	370.02	150.00	1284.00	0.93	0.282	132.00	ND
Nb	0.2	FUS-MS	11.41	11.70	2.48	6.00	15.10	0.93	0.230	8.00	ND
Sn	1	FUS-MS	2.13	2.00	0.64	1.00	4.00	0.61	0.000	1.70	ND
Sb	0.1	INAA	0.72	0.70	0.17	0.30	0.90	0.87	0.040	0.20	2
Cs	0.1	FUS-MS	2.10	1.70	0.97	1.00	3.70	0.87	0.035	2.00	ND
Ba	1	FUS-ICP	460.67	487.00	77.27	335.00	612.00	0.95	0.494	456.00	350
La	0.05	FUS-MS	27.42	28.10	3.24	20.80	32.30	0.90	0.103	20.00	27.8
Ce	0.05	FUS-MS	57.61	59.00	7.43	42.20	67.70	0.92	0.162	43.00	51
Pr	0.01	FUS-MS	6.52	6.76	0.84	4.75	8.01	0.95	0.468	4.90	ND
Nd	0.05	FUS-MS	24.37	24.90	3.15	17.40	29.50	0.93	0.259	20.00	ND
Sm	0.01	FUS-MS	4.88	4.88	0.72	3.43	6.27	0.95	0.584	3.90	ND
Eu	0.005	FUS-MS	1.00	1.00	0.15	0.71	1.22	0.95	0.581	1.10	0.58
Gd	0.01	FUS-MS	4.26	4.39	0.70	2.81	5.53	0.96	0.699	3.70	ND
Tb	0.01	FUS-MS	0.69	0.70	0.10	0.46	0.91	0.95	0.567	0.60	ND
Dy	0.01	FUS-MS	4.24	4.30	0.62	2.70	5.32	0.88	0.053	3.60	ND
Ho	0.01	FUS-MS	0.85	0.86	0.12	0.57	1.07	0.92	0.166	0.77	ND
Er	0.01	FUS-MS	2.54	2.52	0.39	1.63	3.24	0.93	0.246	2.10	ND
Tm	0.005	FUS-MS	0.39	0.39	0.07	0.25	0.50	0.96	0.770	0.28	ND
Yb	0.01	FUS-MS	2.74	2.52	0.49	1.79	3.52	0.94	0.328	1.90	2.2
Lu	0.002	FUS-MS	0.45	0.42	0.08	0.29	0.57	0.94	0.445	0.30	ND
Hf	0.1	FUS-MS	16.52	16.30	9.06	4.40	31.60	0.93	0.303	3.70	10.2
Ta	0.01	FUS-MS	0.98	1.00	0.16	0.62	1.26	0.97	0.790	0.70	0.85
Tl	0.05	FUS-MS	0.24	0.25	0.05	0.15	0.31	0.94	0.434	0.50	ND
Pb	5	TD-ICP	15.07	12.00	7.52	10.00	41.00	0.55	0.000	11.00	105
Th	0.05	FUS-MS	9.90	9.32	2.15	7.35	13.40	0.89	0.065	10.50	5.5
U	0.01	FUS-MS	2.93	2.98	0.47	2.03	3.59	0.95	0.582	2.70	1.8

The results are compared with those published worldwide for the UCC by Rudnick and Gao (2014) and regional published data from dust by Ganor et al. (1991). All contents are expressed in mg/kg except S, and the obtained oxides are given in %

(52.7 ± 22.4 with an interval of 26–94), Cu (29.8 ± 18.8 with a range of 14–94), Zn (72.5 ± 64.8 with a range of 33–226), Y (24.9 ± 3.5 with a range of 18–31), Hf (16.5 ± 9.1 with a range of 4.4–31.6), and Ta (0.98 ± 0.16 with an

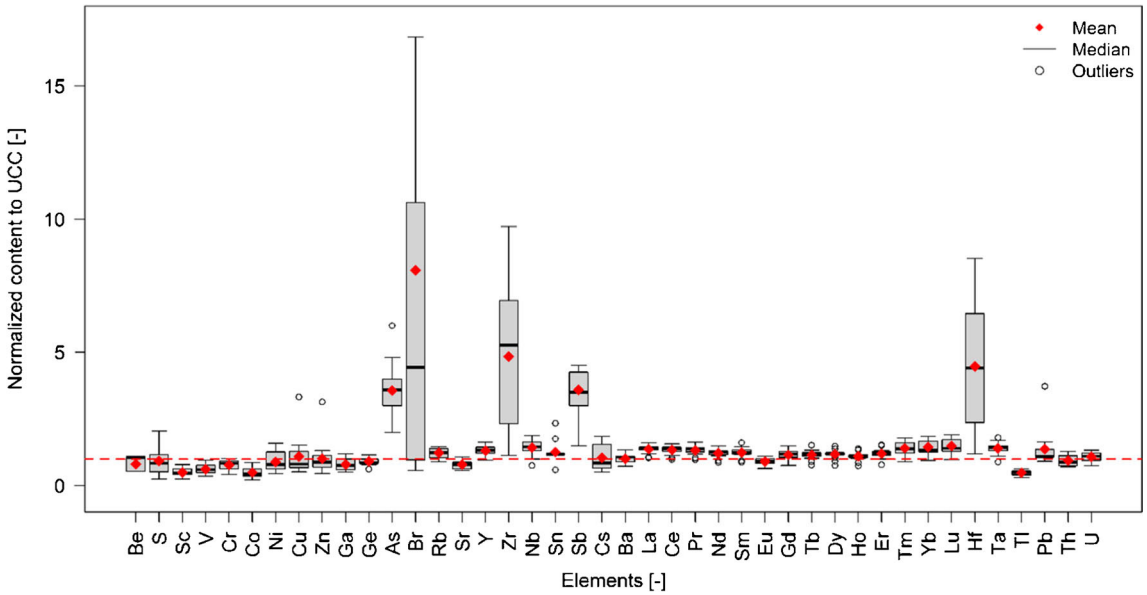

Fig. 2 Box and whisker plot illustrates the normalized content to UCC of 42 elements in the dust samples

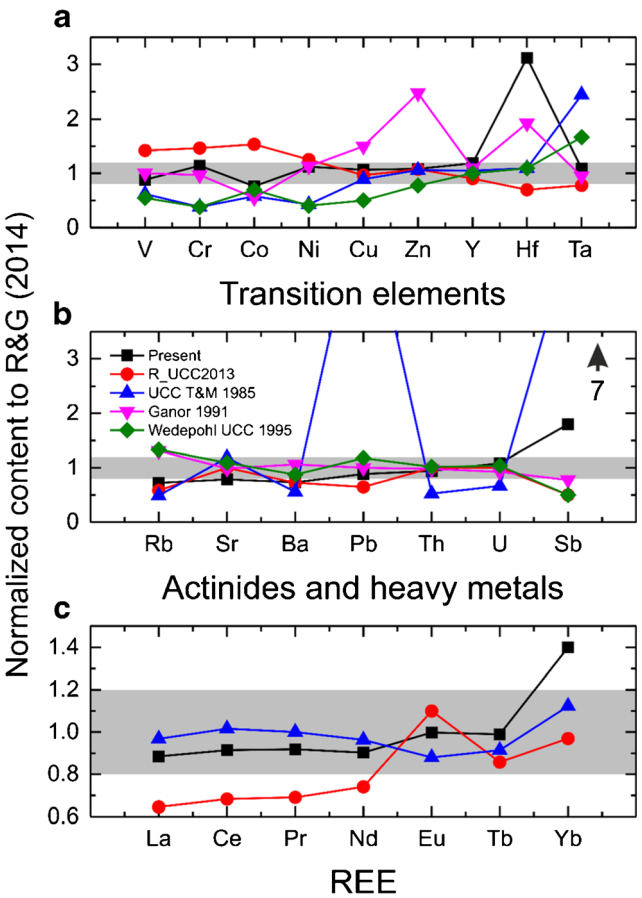

Fig. 3 Comparison of different models for upper-crust composition of the trace elements with studies of airborne dust samples. All values are normalized to the upper-crust composition of Rudnick and Gao (2014). Gray-shaded field represents a ± 20% variation from this value. Trace elements are divided into the following groups: **a** transition metals, **b** actinides and heavy metals, alkali and alkaline earth, and **c** REEs

interval of 0.62–1.26). It is obvious from the figure that there is a significance concentration of Hf.

- The concentrations (mg/kg) of actinides and heavy elements are given for Rb (60.6 ± 8.9 with a range of 44–72), Sr (251.7 ± 48.4 with a range of 182–341), Ba (460.7 ± 77.3 with a range of 335–612), Pb (15.1 ± 7.5 with a range of 10–41), Th (9.9 ± 2 with a range of 7.4–13.4), U (2.9 ± 0.5 with a range of 2.0–3.6), and Sb (0.7 ± 0.1 with a range of 0.3–0.9). The normalized and comparable values are shown in Fig. 3b. The results show that the concentrations of Rb, Ba, Pb, U, and Sb are slight higher than those in UCC, whereas the concentrations of Sr and Th are lower than those in UCC as reported by Rudnick and Gao (2014). It is clear that the data of the present work is in good agreement with those reported regionally and average weighted worldwide by Ganor et al. (1991), Al-Dousari et al. (2016), and Hans Wedepohl (1995), and Rudnick and Gao (2003), respectively.
- A symbiotic behavior of the rare-earth elements compared with the corresponding values in the literature is obviously illustrated in Fig. 3c. The concentration (mg/kg) of La is ranging from 20.8 to 32.3 with an average value of 27.4 ± 3.2, and similarly, the concentration of Ce shows a minimum value of 42.2 and a maximum value of 67.7 with a mean value of 57.6 ± 7.4. Pr concentration is ranging from 4.6 to 8 with a mean value of 6.5 ± 0.8. Nd concentration is ranging from 17.4 to 29.5 with a mean value of 24.4 ± 3.2, likewise for Eu (0.9 ± 0.1 and ranges from 0.7 to 1.2), Tb (0.7 ± 0.1 with a range of 0.5–0.9), and Yb (2.8 ± 0.5 with a minimum value of 1.8 and a maximum value of 3.5). The obtained results are slightly higher than those reported by Taylor and McLennan (1985) and Rudnick

and Gao (2003) with an exception for Eu anomaly, which is slightly lower.

It is apparent from the results that concentrations of Zr are significantly high. This peculiarity was studied by plotting the ratio indicators of Th/Sc (≈ 0.9) versus Zr/Sc (≈ 58.7) as illustrated in Fig. 4. The ratio Th/Sc was compared with the corresponding values (≈ 0.5) by Ganor et al. (1991) and Rudnick and Gao (2014), whereas the Zr/Sc ratio is greater than the corresponding values (≈ 19.5) reported by Badawy et al. (2017) and the world average soil (≈ 22.8) by Kabata-Pendias (2011). Therefore, it can be inferred that significant and high sedimentary recycling was observed. It is clear from Fig. 4 that the source material of these elements is a mixture of UCC and felsic rocks with significant tendency to granite.

The correlation between the concentrations of Th and U in the examined dust samples is presented in Fig. 5. For comparison purposes, other corresponding Th/U ratios were added. For instance, the Th/U ratio of 4.1 was derived by Rudnick and Gao (2014) for UCC, 3.4 was reported by Ganor et al. (1991) for dust, and 3.7 was given by Kabata-Pendias (2011) for world soil average (WSA). To a great extent, the obtained ratio of Th/U for dust samples (3.4 ± 0.5) is almost the same as that obtained by Ganor et al. (1991) for dust. Based on this finding, it could be inferred that the concentration of Th and U in the investigated dust samples is originating from the weathering processes and the anthropological impact is not evidenced.

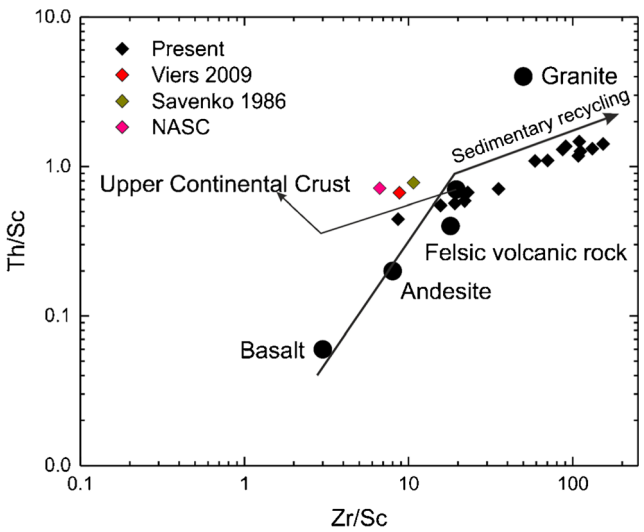

Fig. 4 The Th/Sc vs Zr/Sc biplot illustrating an increased degree of Zr enrichment, proving a high sedimentary recycling, a characteristic for a majority of samples as data confirmed by Gromet et al. (1984), Viers et al. (2009), and Savenko (1986) for North American shale composite (NASC), river sediments, and sediments, respectively. The obtained results show that, most probably, the source material of these elements is a mixture of UCC and felsic rocks with significant tendency are attributed to granite

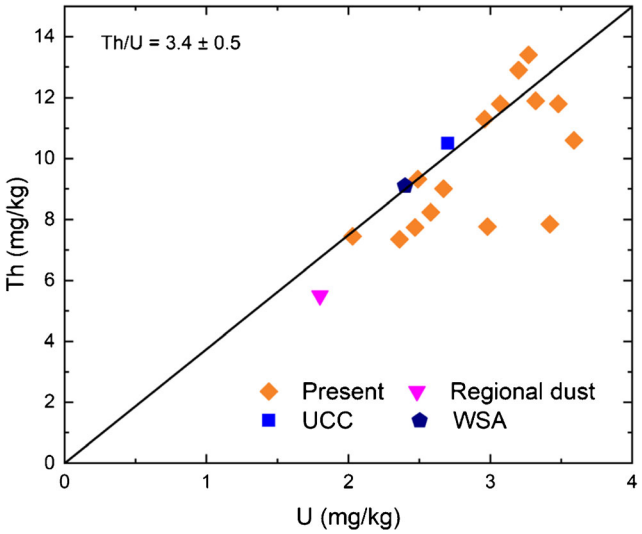

Fig. 5 A plot illustrates the correlation between Th and U in the studied dust samples. For comparison purposes, the corresponding values for the regional study, UCC, and world soil average WSA are added (Ganor 1991; Kabata-Pendias 2011; Rudnick and Gao 2014)

Pollution extent and webs of possible contamination

The EF was calculated for different elements, and the results are stipulated in Table 2. The obtained results of EF are compared with the regional results reported by Ganor et al. (1991) and weighted average worldwide by Rahn et al. (1979). The calculated EFs are lower than the corresponding values reported by Rahn et al. (1979) and in a good matching with the regional results reported by Ganor et al. (1991). The results of EF range from 0.98 to 14.91 for Co and Br, respectively, with a mean value of 3.2. For a better understanding about the pollution extent, the interpretation category of enriched elements and non-enriched ones is given in Table 3. Based on the categories suggested by Ganor et al. (1991), the enrichment factor lower than 2 leads to non-enriched elements and that of more than 7 initiates a significant impact on the human and environment, while the enrichment factor higher than 2 and lower than 7 causes intermediate-enriched elements and investigation process should be launched to get more data on the root cause of the increment to avoid potential consequences. The sorted elements as enriched or non-enriched are summarized as follows:

- A total of 12 elements out of 42 are not enriched, namely Be, S, Sc, V, Cr, Co, Ni, Ga, Ge, Sr, Eu, and Tl, where EF is lower than 2.
- An intermediate-enriched elements are observed for 25 elements, viz. Cu, Zn, Rb, Y, Nb, Sn, Cs, Ba, La, Ce, Pr, Nd, Sm, Gd, Tb, Dy, Ho, Er, Tm, Yb, Lu, Ta, Pb, Th, and U, where EF is higher than 2 and lower than 7.
- Only 5 elements are enriched, namely As, Br, Zr, Sb, and Hf, as their EF is higher than 7. This finding could be due

Table 2 Enrichment factor (EF) compared with the regional and weighted average worldwide (Ganor et al. 1991; Rahn et al. 1979)

Element	Present EF	Ganor et al. (1991)		Rahn et al. (1979)	
		Sahara EF (Fe, rock)	World EF (Al, rock)	Sahara	Worldwide
Be	1.64	0.83	0.83	ND	ND
S	1.97	2.75	2.62	ND	ND
Sc	1.00	0.87	0.62	0.73	1.17
V	1.26	0.79	0.62	0.88	14
Cr	1.63	1.01	0.74	1.02	8.1
Co	0.98	0.26	0.26	0.88	3.5
Ni	1.75	0.72	0.75	2.35	32
Cu	2.33	0.6	0.6	< 20	102
Zn	2.03	2.12	2.12	2.34	260
Ga	1.62	ND	ND	1.94	2.5
Ge	1.92	ND	ND	ND	ND
As	7.27	2.25	2.33	8	310
Br	14.91	4.69	3.53	ND	ND
Rb	2.62	0.82	0.59	1.03	3.4
Sr	1.67	1.25	1.18	ND	ND
Y	2.84	0.97	1.03	ND	ND
Zr	11.55	ND	ND	2.18	1.36
Nb	2.97	ND	ND	ND	ND
Sn	2.73	ND	ND	ND	ND
Sb	7.55	2.02	2.1	5.8	1430
Cs	2.04	ND	ND	1.45	12.4
Ba	2.29	1.03	0.66	2.33	5.5
La	2.93	1.15	1.11	1.78	2.7
Ce	2.85	1.16	1	1.85	2.6
Pr	2.84	ND	ND	ND	ND
Nd	2.59	ND	ND	ND	ND
Sm	2.65	ND	ND	1.68	2.1
Eu	1.91	0.54	0.55	1.73	2.7
Gd	2.43	ND	ND	ND	ND
Tb	2.45	ND	ND	2.02	1.92
Dy	2.50	ND	ND	1.66	2.5
Ho	2.36	ND	ND	ND	ND
Er	2.60	ND	ND	ND	ND
Tm	3.05	ND	ND	ND	ND
Yb	3.14	0.69	0.56	0.91	1.06
Lu	3.27	ND	ND	1.35	1.95
Hf	10.57	2.84	2.23	1.98	2
Ta	3.00	ND	ND	ND	ND
Tl	1.01	ND	ND	ND	ND
Pb	3.08	4.66	4.85	ND	ND
Th	2.09	1.1	0.91	1.92	1.78
U	2.36	0.58	0.28	ND	ND

to the intensely urban extent and anthropological activities in Al-Qassim Region (Jones Lii et al. 2017).

Table 3 Classification of elements by category of enrichment factor values according to Ganor et al. (1991)

EF < 2 non-enriched elements (12)	Be, S, Sc, V, Cr, Co, Ni, Ga, Ge, Sr, Eu, Tl
2 < EF > 7 intermediate elements (25)	Cu, Zn, Rb, Y, Nb, Sn, Cs, Ba, La, Ce, Pr, Nd, Sm, Gd, Tb, Dy, Ho, Er, Tm, Yb, Lu, Ta, Pb, Th, U
EF > 7 enriched elements (5)	As, Br, Zr, Sb, Hf

The average single pollution index was calculated to give an integrative assessment of the contamination. The calculated values show that the PI ranges from a minimum value of 0.74 for location 8 (*Bureydah Center*), while the maximum value was observed for location 5 (*Bureydah South*). The spatial distribution of PI is mapped as shown in Fig. 6.

Findings of dust exposure

In order to assess the human health risk as a result of exposure to metals due to dust inhalation, the HQ was calculated for selected elements, namely carcinogenic Cr, Cr, Co, Ni, Cu, Zn, and Pb. Chemical daily intake (D_{inh}) via inhalation was calculated based on the toxic parameters provided by US EPA (2007) as shown in Table SM1. First, the upper confidence limit content (C_{UCL}) values were calculated and are presented in Table 4. The calculated values of D_{inh} range from 6.8×10^{-10} for Pb to 2.1×10^{-9} for non-carcinogenic Cr with a mean value of $1.3 \times 10^{-9} \pm 6.1 \times 10^{-10}$ mg/kg per day. The obtained results are quite low compared with those published by Kurt-Karakus (2012) for similar elements and almost in line with those published by Mohmand et al. (2015) for

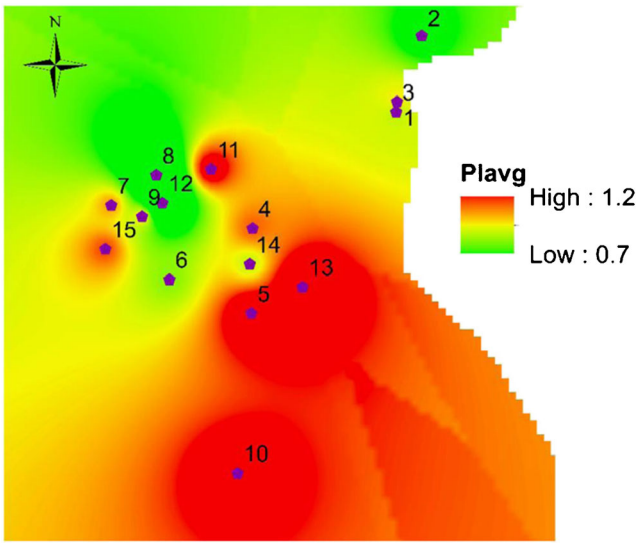

Fig. 6 Spatial map of the average single pollution index illustrates the peak areas

Table 4 Chemical daily intake (CDI_{inh}) and the associated carcinogenic risk (CR) and hazard quotient (HQ) for the selected elements in case of inhalation

Element	*C* (95% UCL) (mg/kg)	R_fD_0 (mg/kg per day)	BAF (%)	SLF (mg/kg per day)	CDI_{inh} (mg/kg per day)	Carcinogenic risk (CR)	Hazard quotient (HQ)
Carcinogenic Cr	17.2		5.83	0.5	6.9×10^{-10}	2.0×10^{-11}	
Cr	17.2	3.0×10^{-3}	5.83		2.1×10^{-9}		4.0×10^{-8}
Co	6.1	3.0×10^{-4}	4.5		7.2×10^{-10}		1.1×10^{-7}
Ni	13.3	2.0×10^{-2}	32.4		1.6×10^{-9}		2.6×10^{-8}
Cu	9.9	4.0×10^{-2}	64.4		1.2×10^{-9}		1.9×10^{-8}
Zn	17.2	3.0×10^{-1}	53.2		2.0×10^{-9}		3.6×10^{-9}
Pb	5.7	3.5×10^{-3}	37.2		6.8×10^{-10}		7.2×10^{-8}

inhaled dust from rural, urban, and industrial areas in Pakistan. The present study is focused only on one exposure pathway. Therefore, in this case, HQ is equal to CR. CR was calculated for carcinogenic Cr to be 2×10^{-11} and showed a low value compared with the corresponding values reported by Kurt-Karakus (2012) (3.4×10^{-10}) and a value of 4.12×10^{-7}, 1.8×10^{-7}, and 1.4×10^{-7} for adult in industrial, urban, and rural areas, respectively, as reported by Mohmand et al. (2015). The obtained results of HQs reveal a mean value of 4.5×10^{-8}, and the calculated standard deviation was 3.8×10^{-8} with a minimum value of 3.6×10^{-9} for Zn and a maximum value of 1.1×10^{-7} for Co. The HQs were calculated for the other elements and are given in descending order as follows: Co > Pb > Cr > Ni > Cu > Zn > carcinogenic Cr. Overall, the obtained results are lower even than the tolerable values as clearly illustrated in Fig. 7. Tolerable values of the carcinogenic health risk index for different trace metals ranged from 1×10^{-6} to 1×10^{-4} (US EPA 2001). Therefore, these elements have no significant health hazard from a point of view of their toxicity and this may be attributed to the decreased concentrations of the considered elements in the dust samples.

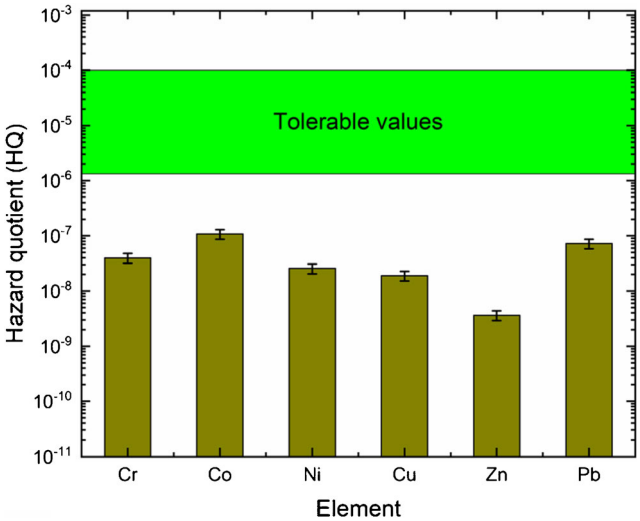

Fig. 7 Hazard quotient of the calculated HQ for the examined elements. Plot illustrates that no significant HQ is observed

Conclusions

The present study outlined the abundances of 42 elements, which were determined in fifteen dust samples collected from Al-Qassim Region, KSA, by means of NAA and ICP-MS. Considerable concentrations of Br, Zr, Hf, As, and Sb were observed. Similarly, EF distinguished the same elements as highly enriched. Ratio indicators of Zr/Sc versus Th/Sc figure out a significant and high tendency of sedimentary recycling in the examined samples. Likewise, the Th/U ratio indicator outlines that no anthropological impact was observed and, most probably, the provenance of these elements is ultimately correlated with UCC. The integrative single pollution index sorted the highest peak value to be *Bureydah South*. Eventually, the present study shows that the calculated values of HQ (4.5×10^{-8}) are significantly lower than the tolerable values (1×10^{-6} to 1×10^{-4}).

Funding information The authors extend their appreciation to the Deanship of Scientific Research at King Khalid University for funding this work through the research group program under grant number R.G.P.1/118/40.

References

A.S.T.M. Standard D-1739-70 (1979) American Society for Testing and Materials, part 23. Philadelphia, PA

Abrahim GMS, Parker RJ (2008) Assessment of heavy metal enrichment factors and the degree of contamination in marine sediments from Tamaki Estuary, Auckland, New Zealand. Environ Monit Assess 136:227–238. https://doi.org/10.1007/s10661-007-9678-2

Al-Awadhi JM, Al-Dousari AM, Khalaf FI (2014) Influence of land degradation on the local rate of dust fallout in Kuwait. Atmos Clim Sci 04:437–446. https://doi.org/10.4236/acs.2014.43042

Al-Dousari A (2005) Causes and indicators of land degradation in the north-western part of Kuwait. Arab Gulf J Sci Res 23:69–79

Al-Dousari AM (2009) Recent studies on dust fallout within preserved and open areas in Kuwait. In: Bhat NR Al-Nasser A OS (ed) Desertification in arid lands. Institute for Scientific Research, Kuwait, pp 137–147

Al-Dousari AM, Aba A, Al-Awadhi S, Ahmed M, Al-Dousari N (2016) Temporal and spatial assessment of pollen, radionuclides, minerals

and trace elements in deposited dust within Kuwait. Arab J Geosci 9: 95. https://doi.org/10.1007/s12517-015-2182-z

Al-Dousari A, Doronzo D, Ahmed M (2017) Types, indications and impact evaluation of sand and dust storms trajectories in the Arabian Gulf. Sustainability 9. https://doi.org/10.3390/su9091526

Al-enezi E, Al-Dousari A, Al-shammari F (2014) Modeling adsorption of inorganic phosphorus on dust fallout in Kuwait bay. J Eng Res 2:1–14. https://doi.org/10.7603/s40632-014-0001-4

Al-Ghadban A, Uddin S, Beg M, Al-Dousari A, Gevao B, al-Yamani F (2008) Ecological consequences of river manipulations and drainage of Mesopotamian marshes on the Arabian Gulf ecosystem: investigations on changes in sedimentology and environmental quality, with special reference to Kuwait Bay vol 9362. Institute for Scientific Research, Kuwait. https://doi.org/10.13140/RG.2.2.10969.62562

Alharbi A, El-Taher A (2016) Elemental analysis of basalt by instrumental neutron activation analysis and inductively coupled plasma mass spectrometer. J Environ Sci Technol 9:335–339. https://doi.org/10.3923/jest.2016.335.339

Al-Taani AA, Nazzal Y, Howari FM (2019) Assessment of heavy metals in roadside dust along the Abu Dhabi–Al Ain National Highway, UAE. Environ Earth Sci 78:411. https://doi.org/10.1007/s12665-019-8406-x

Amato F et al (2009) Quantifying road dust resuspension in urban environment by multilinear engine: a comparison with PMF2. Atmos Environ 43:2770–2780. https://doi.org/10.1016/j.atmosenv.2009.02.039

Badawy W, Chepurchenko OY, El Samman H, Frontasyeva MV (2016) Assessment of industrial contamination of agricultural soil adjacent to Sadat City, Egypt. Ecol Chem Eng S 23:297–310. https://doi.org/10.1515/eces-2016-0021

Badawy WM, Ghanim EH, Duliu OG, El Samman H, Frontasyeva MV (2017) Major and trace element distribution in soil and sediments from the Egyptian central Nile Valley. J Afr Earth Sci 131:53–61. https://doi.org/10.1016/j.jafrearsci.2017.03.029

Beavington F, Cawse PA (1979) The deposition of trace elements and major nutrients in dust and rainwater in northern Nigeria. Sci Total Environ 13:263–274. https://doi.org/10.1016/0048-9697(79)90106-2

Blott SJ, Al-Dousari AM, Pye K, Saye SE (2004) Three-dimensional characterization of sand grain shape and surface texture using a nitrogen gas adsorption technique. J Sediment Petrol 74:156–159. https://doi.org/10.1306/052403740156

Dan J (1990) The effect of dust deposition on the soils of the land of Israel. Quat Int 5:107–113. https://doi.org/10.1016/1040-6182(90)90030-8

Davis JC (2002) Statistics and data analysis in geology. J Geol 2:656

Doronzo MD, Al-Dousari A (2019) Preface to dust events in the environment. Sustainability 11. https://doi.org/10.3390/su11030628

Doronzo DM, Al-Dousari A, Folch A, Dagsson-Waldhauserova P (2016) Preface to the dust topical collection. Arab J Geosci 9:468. https://doi.org/10.1007/s12517-016-2504-9

El-Taher A, Khater AEM (2016) Elemental characterization of Hazm El-Jalamid phosphorite by instrumental neutron activation analysis. Appl Radiat Isot 114:121–127

El-Taher A, Kratz KL, Nossair A, Azzam AH (2003) Determination of gold in two Egyptian gold ores using instrumental neutron activation analysis. Radiat Phys Chem 68:751–755. https://doi.org/10.1016/S0969-806X(03)00401-8

Ganor E (1991) The composition of clay minerals transported to Israel as indicators of Saharan dust emission. Atmos Environ Part A 25: 2657–2664. https://doi.org/10.1016/0960-1686(91)90195-D

Ganor E, Mamane Y (1982) Transport of Saharan dust across the eastern Mediterranean. Atmos Environ (1967) 16:581–587. https://doi.org/10.1016/0004-6981(82)90167-6

Ganor E, Foner HA, Brenner S, Neeman E, Lavi N (1991) The chemical composition of aerosols settling in Israel following dust storms. Atmos Environ Part A 25:2665–2670. https://doi.org/10.1016/0960-1686(91)90196-E

Gilbert RO (1987) Statistical methods for environmental pollution monitoring. Wiley, Van Nostrand Reinhold, New York

Gromet LP, Haskin LA, Korotev RL, Dymek RF (1984) The "North American shale composite": its compilation, major and trace element characteristics. Geochim Cosmochim Acta 48:2469–2482. https://doi.org/10.1016/0016-7037(84)90298-9

Hammer Ø, Harper DAT, Ryan PD (2001) Paleontological statistics software package for education and data analysis. Palaeontol Electron 4: 9

Hans Wedepohl K (1995) The composition of the continental crust. Geochim Cosmochim Acta 59:1217–1232. https://doi.org/10.1016/0016-7037(95)00038-2

Hoffman EL (1992) Instrumental neutron activation in geoanalysis. J Geochem Explor 44:297–319. https://doi.org/10.1016/0375-6742(92)90053-B

Jeddah Regional Centre for Climate (JRCC) (2015) Drought monitoring report. The General Authority of Meteorology and Environmental Protection. https://www.pme.gov.sa/En/Meteorology/National_Centre_Meteorology/Pages/JRCC.aspx. Accessed Jan 2019

Jones III JV, Piatak NM, Bedinger GM (2017) Zirconium and hafnium. Reston, VA. https://doi.org/10.3133/pp1802V

Kabata-Pendias A (2011) Trace elements in soils and plants. CRC, Boca Raton, pp 1–534. https://doi.org/10.1201/b10158-25

Khan NY et al (1999) Assessment of sediment quality in Kuwait's territorial waters. Phase 1: Kuwait Bay. Institute for Scientific Research, Kuwait

Kurt-Karakus PB (2012) Determination of heavy metals in indoor dust from Istanbul, Turkey: estimation of the health risk. Environ Int 50: 47–55. https://doi.org/10.1016/j.envint.2012.09.011

Lv J, Liu Y, Zhang Z, Zhou R, Zhu Y (2015) Distinguishing anthropogenic and natural sources of trace elements in soils undergoing recent 10-year rapid urbanization: a case of Donggang, Eastern China. Environ Sci Pollut Res 22:10539–10550. https://doi.org/10.1007/s11356-015-4213-4

Mohmand J et al (2015) Human exposure to toxic metals via contaminated dust: bio-accumulation trends and their potential risk estimation. Chemosphere 132:142–151. https://doi.org/10.1016/j.chemosphere.2015.03.004

Mustafa MM, El Behiry A, El Mossad YM (2016) Al-Qassim industrial area and its role in changing the diseases patterns among workers over the past five years (2011-2015). Int J Community Med Public Health 3:9. https://doi.org/10.18203/2394-6040.ijcmph20164276

Norouzi S, Khademi H, Faz Cano A, Acosta JA (2015) Using plane tree leaves for biomonitoring of dust borne heavy metals: a case study from Isfahan, Central Iran. Ecol Indic 57:64–73. https://doi.org/10.1016/j.ecolind.2015.04.011

Qingjie G, Jun D, Yunchuan X, Qingfei W, Liqiang Y (2008) Calculating pollution indices by heavy metals in ecological geochemistry assessment and a case study in parks of Beijing. J China Univ Geosci 19: 230–241. https://doi.org/10.1016/S1002-0705(08)60042-4

R Core Team (2016) R: A language and environment for statistical computing. R Foundation for Statistical Computing, Vienna

Rahn KA, Borys RD, Shaw GE, Schutz L (1979) Long-range impact of desert aerosol on atmospheric chemistry: two examples. In: Morales C (ed) Scope 14: Saharan dust (mobilization, transport, deposition). In. Wiley, Chichester, pp 243–266

Reimann C, de Caritat P (2005) Distinguishing between natural and anthropogenic sources for elements in the environment: regional geochemical surveys versus enrichment factors. Sci Total Environ 337: 91–107. https://doi.org/10.1016/j.scitotenv.2004.06.011

Rudnick RL, Gao S (2003) Composition of the continental crust. Treatise on Geochemistry 3:1–64. https://doi.org/10.1016/B0-08-043751-6/03016-4

Rudnick RL, Gao S (2014) 4.1—composition of the continental crust A2—Holland, Heinrich D. In: Turekian KK (ed) Treatise on geochemistry, 2nd edn. Elsevier, Oxford, pp 1–51. https://doi.org/10.1016/B978-0-08-095975-7.00301-6

Rydell HS, Prospero JM (1972) Uranium and thorium concentrations in wind-borne Saharan dust over the Western Equatorial North Atlantic Ocean. Earth Planet Sci Lett 14:397–402. https://doi.org/10.1016/0012-821X(72)90140-9

Savenko SV (1986) Geochemical aspects of biosedimentation. Dokladi, An SSSR 288:1192–1196

Shaltout AA, Khoder MI, El-Abssawy AA, Hassan SK, Borges DLG (2013) Determination of rare earth elements in dust deposited on tree leaves from Greater Cairo using inductively coupled plasma mass spectrometry. Environ Pollut 178:197–201. https://doi.org/10.1016/j.envpol.2013.03.044

Shapiro SS, Wilk MB (1965) An analysis of variance test for normality (complete samples). Biometrika 52:591–611. https://doi.org/10.1093/biomet/52.3-4.591

Subramaniam N, Al-Sudairawi M, Al-Dousari A, Al-Dousari N (2015) Probability distribution and extreme value analysis of total suspended particulate matter in Kuwait. Arab J Geosci 8:11329–11344. https://doi.org/10.1007/s12517-015-2008-z

Taylor SR, McLennan SM (1985) The continental crust, its composition and evolution: an examination of the geochemical record preserved in sedimentary rocks. Blackwell Scientific, Oxford

US EPA (1996) Soil screening guidance: technical background document. EPA/540/R-95/128. Office of Solid Waste and Emergency Response. U.S. Environmental Protection Agency, Washington, D.C

US EPA (2001) Risk assessment guidance for Superfund: volume III part A, process for conducting probabilistic risk assessment. US Environmental Protection Agency, Washington, D.C

US EPA (2007) In: U.S. Environmental Protection Agency (ed) Estimation of relative bioavailability of lead in soil and soil-like materials using in vivo and in vitro methods. Office of Solid Waste and Emergency Response, Washington, D.C

US EPA (2010) Region 9, Regional screening levels tables. http://www.epa.gov/region9/superfund/prg/index.html. Jan 2019

Van den Berg R (1995) Human exposure to soil contamination: a qualitative and quantitative analysis towards proposals for human toxicological intervention values. RIVM Report no. 725201011. National Institute of Public Health and Environmental Protection (RIVM), Bilthoven

Viers J, Dupre B, Gaillardet G (2009) Chemical composition of suspended sediments in World Rivers: new insights from a new database. Sci Total Environ 407:853–868. https://doi.org/10.1016/j.scitotenv.2008.09.053

Whicker JJ, Pinder JE, Breshears DD, Eberhart CF (2006) From dust to dose: effects of forest disturbance on increased inhalation exposure. Sci Total Environ 368:519–530. https://doi.org/10.1016/j.scitotenv.2006.03.003

Zheng N, Liu J, Wang Q, Liang Z (2010) Health risk assessment of heavy metal exposure to street dust in the zinc smelting district, northeast of China. Sci Total Environ 408:726–733. https://doi.org/10.1016/j.scitotenv.2009.10.075